Rev. Roum. Sci. Techn.– Électrotechn. et Énerg.
Vol. **69**, *1*, pp. 9–14, Bucarest, 2024

TUNING OF PI SPEED CONTROLLER IN DIRECT TORQUE CONTROL OF DUAL STAR INDUCTION MOTOR BASED ON GENETIC ALGORITHMS AND NEURO-FUZZY SCHEMES

RAHMA BELAL, MOHAMMED FLITTI, MOHAMMED LAMINE ZEGAI

Keywords: Dual star induction machine (DSIM); Adaptive neuro-fuzzy inference systems (ANFIS); Genetic algorithm (GA); Direct torque control (DTC); Proportional integral controller (PI); Inverter.

Thanks to the positive characteristics of the double stator machine (DSIM), its high reliability, and reduced rotor torque ripples, it has become among the most important multiphase machines included in industrial applications. This article aims to apply the two techniques of artificial intelligence represented by the adaptive neuro-fuzzy inference systems (ANFIS) and the genetic algorithm (GA) for direct torque control (DTC) of the DSIM to improve the performance of the machine. The ability to learn and the parallelism of operation characteristics made exploiting the GA to control the machine possible instead of using the proportional integral controller (PI). Fixed switching frequency obtained, given with the vector selection table and hysteresis, allowed the inclusion of the ANFIS technique in the DTC strategy. Two-level inverters are included to feed the DSIM. Several results prove that the two techniques applied, ANFIS and GA, improve the quality of the electromagnetic torque and flux and the dynamic responses of the DSIM.

1. **INTRODUCTION**

The ever-increasing number of electrical machines permeating more and more aspects of human life is leading to increased attention regarding the noise they generate. Particularly due to the transformation of the energy system and the associated increase in the use of synchronous electrical machines in applications with a high-power density (*e.g*., wind energy and traction drives, electric vehicles, or electric aircraft...), multi-phase machines are now a strong focus of noise-reduction [1]. As [2,3] describe, doubly star (double stator) induction machines are one of the most widely used machines in many sectors of the industry due to their several advantages compared to conventional three-phase induction motors, such as higher efficiency, minimized rotor harmonic currents, reduced torque pulsations, reliability, and fault tolerance capability.

The dual star induction machine (DSIM), also named dual three-phase induction machine (DTPIM), has a structure that comprises in the stator two three-phase winding systems coupled in a star out of phase between them of an angle pi/6 and a rotor wound in a squirrel cage. To simplify the study, we consider the electric circuits of the rotor to be equivalent to a three-phase winding in a short circuit.

Direct torque control (DTC) is a well-known strategy in electrical engineering. Lately, it has increasingly been used in industrial applications, compared to other kinds of control, particularly vector control. The DTC is much less sensitive to parametric variations that reduce the system's performance to be controlled, and it also allows very fast dynamic torque responses [4]; despite its simplicity, DTC allows good torque control in steady state and transient operating conditions to be obtained. However, hysteresis controllers for flux and torque lead to torque and current ripple and variable switching frequency operation for the voltage source inverter. Several papers discussed different solutions to deal with these problems. In [5], the authors aim for a five-level DTC-SVM method with an efficient dc voltage balancing control method dedicated to a double-star induction machine. In [6], the paper presents the direct torque control (DTC) of a dual star induction machine (DSIM) employing a sliding mode speed controller; in [7] the research proposes a modified direct torque control to minimize the harmonics of the stator current and reduce ripples, the hysteresis controllers of the electrometric torque are instead by a developed 5-level regulator based on more vector voltages to reduce the torque ripples and the error torque. In addition, a PI controller is incorporated into the 5-level regulator to improve the torque response. Recent attention has been given to combining artificial intelligent control techniques with a DTC scheme for improved performance and enhanced robustness [8]. In [9,10], artificial intelligence was used with DTC.

The objective of the proposed control strategy is to drive the dual-star asynchronous induction motor using the Direct Torque Control (DTC) technique. Additionally, this strategy aims to replace the conventional switching table in our control system with another intelligent table based on neuro-fuzzy techniques, utilizing the ANFIS GUI tool interface for optimal vector selection to power the DSIM motor. Furthermore, the PI speed controller is replaced by a new intelligent technique using a tool presented within the genetic algorithm to reduce torque errors at low and high speeds. A study on harmonic distortion (THD) was also conducted for DSIM.

2. **DSIM MODELING**

The electrical supply for the double-star induction machine, operating in motor mode and variable speed, is provided by two voltage source inverters that are mutually connected to the winding of the stator.

The dual star asymmetric induction motor comprises two sets of three-phase star-connected stator wings spaced electrically at 30° (Fig. 1); the rotor can be a short-circuited three-phase winding one or a squirrel cage one. A wound rotor is considered here [11–13] for simplicity.

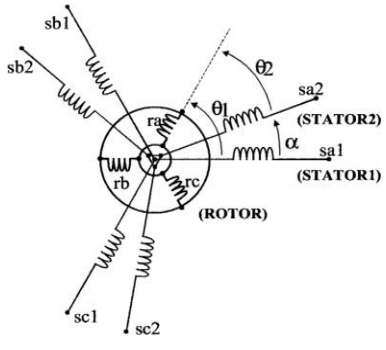

Fig. 1 – Windings of DSIM.

Department of Electrical Engineering, University of Blhadj Bouchaib, Ain Temouchent, BP. 284,46000, Algeria
E-mails: rahma.belal@univ-temouchent.edu.dz, mohammed.flitti@univ-temouchent.edu.dz, mohamedamine.zegai@univ-temouchent.edu.dz.

DOI: 10.59277/RRST-EE.2023.69.1.2

To derive the model, the following general assumptions are made:

- motor windings are equivalent, sinusoidally field distributed;
- both stars have the same parameters;
- flux path is linear;
- magnetic saturation effects are negligible;
- magnetic hysteresis is negligible.

The mathematical model can be derived from the three-phase model by walking the Concordia hypotheses while the slot effect of DSIM is ignored, the core less, the saturation, in a stationary reference frame. As seen in eq. (1)–(10) the DSIM model may be stated as follows:

- Electric equations:

$$V_{s\alpha 1,2}=R_s i_{s\alpha 1,2}+\frac{d\varphi_{s\alpha 1,2}}{dt}, \quad (1)$$

$$V_{s\alpha 1,2}=R_s i_{s\alpha 1,2}+\frac{d\varphi_{s\alpha 1,2}}{dt}, \quad (2)$$

$$V_{r\alpha}=R_r i_{r\alpha}+\frac{d\varphi_{r\alpha}}{dt}-(\omega_s-\omega_r)\varphi_{r\beta}, \quad (3)$$

$$V_{r\beta}=R_r i_{r\beta}+\frac{d\varphi_{r\beta}}{dt}-(\omega_s-\omega_r)\varphi_{r\alpha}, \quad (4)$$

- Magnetic equation:

$$\varphi_{s\alpha 1,2}=L_s i_{s\alpha 1,2}+L_m i_{r\alpha}, \quad (5)$$

$$\varphi_{s\beta 1,2}=L_s i_{s\beta 1,2}+L_m i_{r\beta}, \quad (6)$$

$$\varphi_{r\alpha}=L_r i_{r\alpha}+L_m i_{r\alpha}, \quad (7)$$

$$\varphi_{r\beta}=L_r i_{r\beta}+L_m i_{r\beta}, \quad (8)$$

- Mechanical equations:

$$T_{em}=p\,(\varphi_{s\alpha 1} i_{s\beta 1}-\varphi_{s\beta 1} i_{s\alpha 1})+(\varphi_{s\alpha 2} i_{s\beta 2}-\varphi_{s\beta 2} i_{s\alpha 2}), \quad (9)$$

$$\frac{d\Omega_r}{dt}=T_{em}-T_r-f_r\Omega_r. \quad (10)$$

3. DTC STRATEGY

The fundamental idea behind the DTC concept is to achieve decoupled control of both flux and torque by properly selecting the stator voltage analogous to the torque and flux error, and this choice is based on the utilization of hysteresis controllers, the outputs of the hysteresis regulators when combined with information about the flux position, determine the optimal voltage vectors. These vectors enable the inverter VSI to reach seven distinct phase-plane positions, which correspond to the inverter output voltage vector's eight sequences [8,14,27].

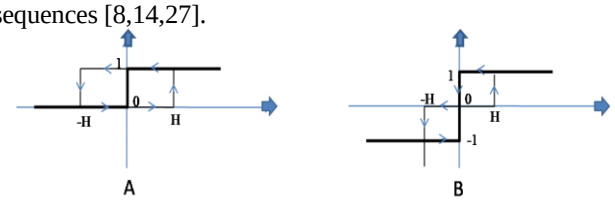

Fig. 1 – Flux hysteresis comparator (A), torque hysteresis comparator (B).

The stator and rotor (α,β) fluxes' magnitudes can be evaluated as follows. The expression of the stator flux is given by:

$$\varphi_{s\alpha 1,2}=\int_0^t (V_{s\alpha}-R_s i_{s\alpha 1,2})dt, \quad (11)$$

$$\varphi_{s\beta 1,2}=\int_0^t (V_{s\beta}-R_s i_{s\beta 1,2})dt. \quad (12)$$

The sectors of the fluxes are divided into six sectors, each covering an angle π/3 and represented in a complex two-dimensional plane. The location of the space vector of fluxes in the complex plane can be represented as follows [14,23]

$$\theta_{s1,2}=\arctan\left(\frac{\varphi_{s\beta 1,2}}{\varphi_{s\alpha 1,2}}\right). \quad (13)$$

To exploit the operation possible sequences of the inverter on two levels, the classical selection table of the DTC is summarized in Table 1. It shows the commutation strategy suggested by Takahashi, to control the stator flux and the electromagnetic torque of the induction motor [15].

Table 1

Applied selected voltage vectors

$\Delta\varphi_s$	ΔC_e	Sector 1	2	3	4	5	6
1	1	V_2 1,1,0	V_3 0,1,0	V_4 0,1,1	V_5 0,0,1	V_6 1,0,1	V_1 1,0,0
	0	V_7 1,1,1	V_0 0,0,0	V_7 1,1,1	V_0 0,0,0	V_7 1,1,1	V_0 0,0,0
	-1	V_6 1,0,1	V_1 1,0,0	V_2 1,1,0	V_3 0,1,0	V_4 0,1,1	V_5 0,0,1
0	1	V_3 0,1,0	V_4 0,1,1	V_5 0,0,1	V_6 1,0,1	V_1 1,0,0	V_2 1,1,0
	0	V_0 0,0,0	V_7 1,1,1	V_0 0,0,0	V_7 1,1,1	V_0 0,0,0	V_7 1,1,1
	-1	V_5 0,0,1	V_6 1,0,1	V_1 1,0,0	V_2 1,1,0	V_3 0,1,0	V_4 0,1,1

The whole system consists of control DTCs coupled to the DSIM, influenced by speed and torque references:

1. Apply a speed step of 300 rad/s from 0 s to 5 s.
2. During the speed change process, the load torque is applied to the system, starting from the rated load torque jump of 10 Nm for 2.5 s, then the motor keeps idling.

At the beginning of the system operation, the following parameters were set sampling frequency: $f_S = 0.001$ Hz ; width of the hysteresis band:

$$\Delta T_{em} = \pm 0.5 \text{ Nm}, \ \Delta\varphi_s = \Delta\varphi_r = \pm 0.01 \text{ Wb}.$$

Figure 3 shows the stator voltages delivered by the voltage inverters; the voltages are of the two-level type. Figures 4 and 5 illustrate the stator currents and their THDs, determining the harmonic rate when using the DTC. It should be noted that the currents are of sinusoidal form, which are harmonics of the THD values of 6.37 %. If the THD rate is high, we will see more ripples in the torque, decreasing the motor's lifetime.

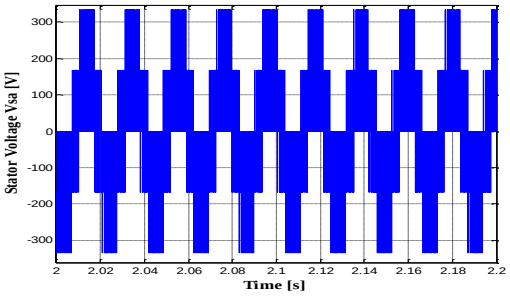

Fig. 3 – Stator Voltage Vsa of the DTC.

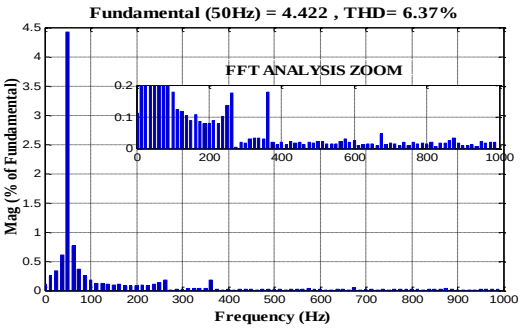

Fig. 4 – Stator current THD of the DTC.

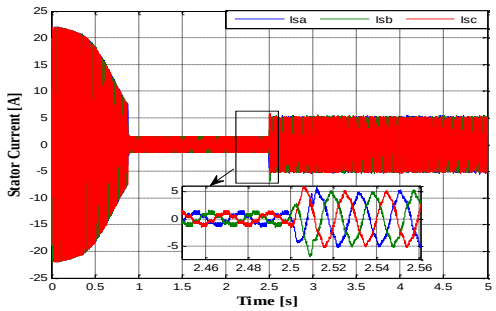

Fig. 5 – Stator currents of the DTC.

4. DTC WITH NEURO-FUZZY

The essential part of neuro-fuzzy inference comes from a common framework called adaptive networks, which unifies neural networks and fuzzy logic [16].

Hybrid neuro-fuzzy networks learn from reports and models using a supervised learning algorithm that examines data across a set of training that consists of sample entries and their associated outputs.

During the learning phase, a hybrid neuro-fuzzy network modifies its internal structure to reflect the ratio of inputs to outputs throughout the training (knowledge base). The accuracy of a neuro-fuzzy network is checked after the learning cycle is complete using a separate set of inputs and outputs called the whole validation [17].

In this paper, we applied the distinguished adaptive neuro-fuzzy inference system (ANFIS) of the type of integrated hybrid neuro-fuzzy system instead of the conventional switching table to control the suitable selection vector. The training of the adapter is done through the error backpropagation algorithm to optimize the parameters of the premise parts to produce the knowledge base automatically and the resolution of the consequent parameters by the least squares method (hybrid learning) [17,18]. The equivalent neuronal structure proposed in Matlab is shown in (Fig. 6).

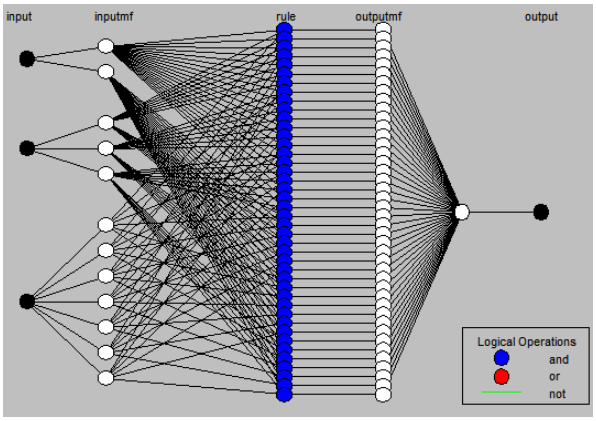

Fig. 6 – Topology of the neuro-fuzzy model used.

The structure proposed contains five network layers:

Layer 1: It is the input layer, the adaptation of the parameters of the antecedents to make their fuzzification.

Layer 2: This is the trigger force layer of the rules, as each neuron in this layer corresponds to a simple fuzzy rule and calculates the implementation force of the rule it represents.

Layer 3: This is the normalization layer of the triggering forces. Each neuron in this layer receives entries from all neurons in the ruler layer.

Layer 4: This defuzzification layer adapts the consequent parameters; each neuron in this layer is connected to the respective normalizing neuron and receives the initial inputs.

Layer 5: This is the final output layer of all defuzzification neurons; this layer sums up all the incoming signals.

Table 2

Parameters setting for ANFIS model

ANFIS setting	Parameters
Input variables	Stator flux error, electromagnetic torque error and Sector
Output variables	Selection voltage vector
Type of input MFs	Gauss MF
Type of output MFs	Linear
Type inference	Sugeno
Number of rule	42 rules
Deffuzification	Wtaver

5. GENETIC ALGORITHM CONTROLLER

Genetic algorithms (abbreviation GA) are an optimization method based on natural selection and natural genetic mechanisms in biology. Because it uses group search and crossover operator (see Fig. 7) and mutation operator to exchange information between individuals, it has implicit parallelism, greatly improving search efficiency, and overcomes the continuous and differentiable requirements of traditional optimization methods for objective functions. Therefore, GA is the best way to control this compromise; it is widely used in scientific research and practical problems, and the fittest potential solutions are developed to produce even more optimal ones. Each string (chromosome) is a possible solution to the problem being optimized, and each bit (or group of bits) represents a value or some variable of the problem (gene) well. For the implementation of the GAs, we used tournament selection, arithmetic crossover, and mutation [19,20,26].

Though genetic algorithms act subtly, the basic execution cycle, the "central loop," is quite simple [21]:

Step 1. From the set of classifiers, select pairs according to strength – the stronger the classifier, the more likely its selection.

Step 2. Apply genetic operators to the pairs, creating "offspring" classifiers. Cross-over is chief among the genetic operators, which exchanges a randomly selected segment between the pairs.

Step 3. Replace the weakest classifiers with the offspring.

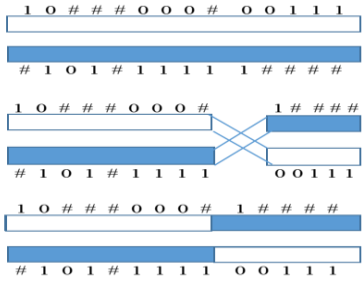

Fig. 7 – Example of the crossover operator.

We note that several performance indices are developed:

The integral of squared error (ISE)

$$I_1 = \int_0^\infty e^2(t)\mathrm{d}t.$$

The integral of absolute Error (IAE)

$$I_2 = \int_0^\infty |e(t)|\mathrm{d}t.$$

The integral of time multiply squared error (ITSE)

$$I_3 = \int_0^{\infty} te^2(t)\mathrm{d}t.$$

The integral of time multiply absolute error (ITAE)

$$I_4 = \int_0^{\infty} t|\mathrm{e}(t)|\mathrm{d}t.$$

The speed is controlled by a PI controller in a traditional DTC control of undesired overshoots and static errors in non-linear systems. However, the DTC's inadequacies cannot address this case [22]. The GA's optimization of the parameters KP, KI, and KD allows for the creation of ideal PI controller values at each sample time that are tailored to the system's nonlinearity. In our work, the performance index applied is ITSE. The optimized design of this regulator is done by a strategy consisting of a GA to precisely locate the global minimum using the 'Gatool' window under Matlab [23]. Figure 8 (Table 3), illustrates the gains synthesized by the conventional DTC, as well as the optimal optimizer gains by the GA algorithm. The parameters of the algorithm used are:

- population size is 30;
- tournament type selection;
- the arithmetic function is used in the crossover;
- the adaptive feasible function is used for mutation;
- the number of generations is 26.

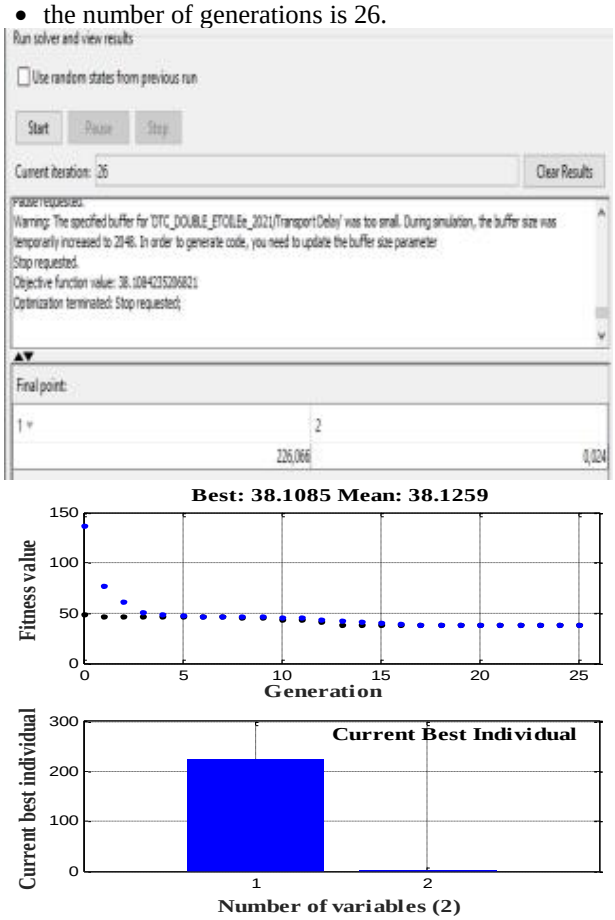

Fig. 8 – The best fitness and best individual of GA_DSIM.

Table 3

Synthesis and optimized PI gains for DTC and GA_DTC

Controller parameters	DTC	GA_DTC
K_p	1500	226.066
K_i	20	0.024

The block diagram of a GA/NF-DTC controlled DSIM by a 2-level inverter is shown in Fig. 9.

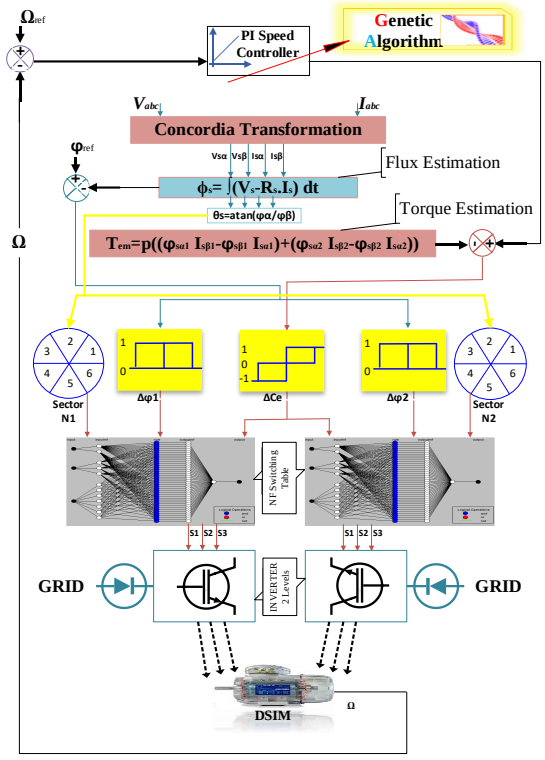

Fig. 9 – NF-DTC control schematic applied to DSIM.

6. SIMULATION RESULT

In Fig. 10, both responses from the torque of C-DTC (conventional) and GA/NF_DTC (genetic algorithm-neuro-fuzzy based direct torque control) will exhibit consistent tracking of the full load torque reference throughout the test. These responses represent an initial torque up to 30 Nm, expected due to current requirements at the start of rotation and during acceleration. We observe a drop in torque presented by the DTC, which the proposed GA-DTC corrects. Notably, at 2.5 s, the electromagnetic torque peaks when subjected to a 10 Nm load, after which it maintains a constant value of 10 Nm.

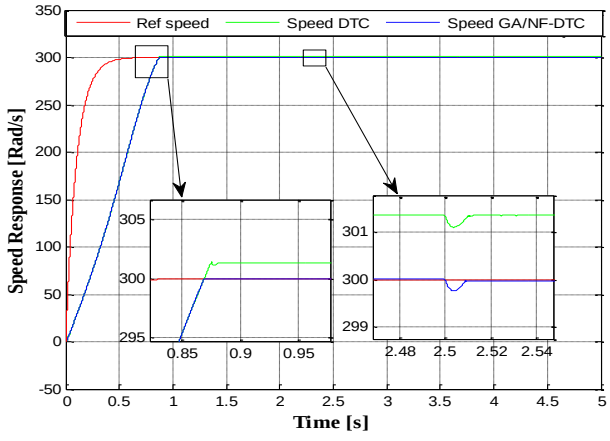

Fig. 10 – Speed responses of both strategies C-DTC and GA/NF_DTC.

To verify the proposed techniques in this paper, a digital simulation based on the Matlab/Simulink program with ANFISToolbox and GA Gatool is used to simulate the GA/NF_DTC, as shown in Figs. 11–15.

Moving on to Fig. 11, it illustrates the speed performance of the DSIM. The speed C-DTC is green, indicating reference tracking throughout the 300 rad/s reference point. However,

an overshoot in speed is addressed using the GA (depicted in blue within the same figure), as highlighted in the zoomed-in section. At 2.5 s, a speed drop is caused by adding a 10 Nm load. Notably, the motor speed maintains its reference value with the presence of a speed controller. The rapid response of DTC_GA/NF demonstrates absolute reference tracking without overshoot or static error. Indeed, Fig. 15 is a confirmation of our arguments.

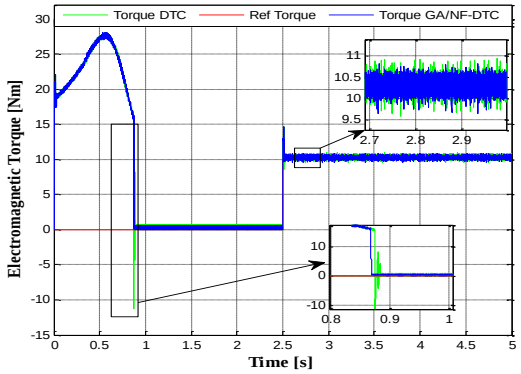

Fig. 11 – Electromagnetic torque of the DTC and GA/NF_DTC.

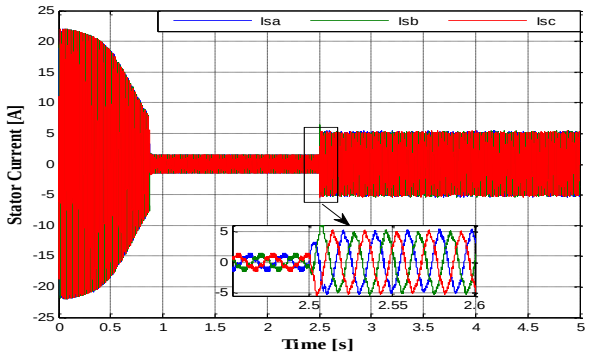

Fig. 12 – Stator currents of the GA/NF_DTC.

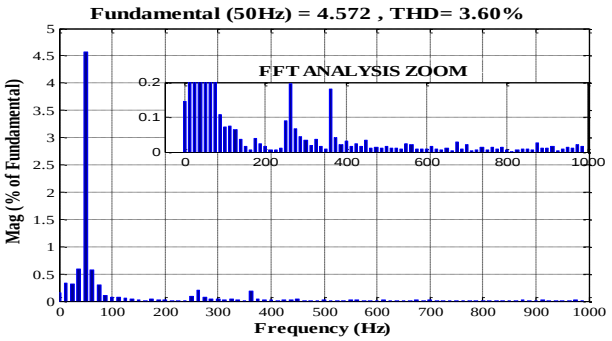

Fig. 13 – Stator current THD of the GA/NF_DTC.

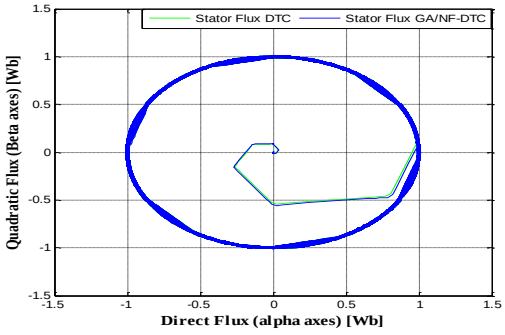

Fig. 14 – Stator flux of the GA/NF_DTC.

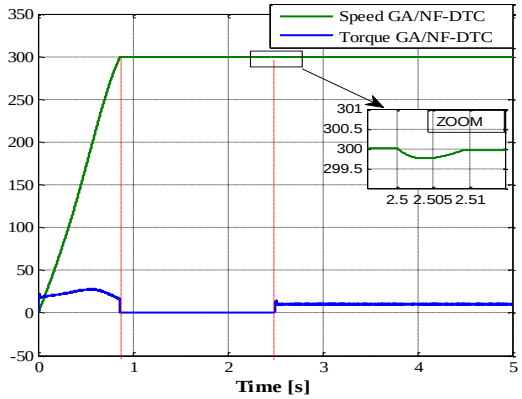

Fig. 15 – Speed and electromagnetic torque of GA/NF_DTC.

Figures 12 and 13 illustrate the stator currents of GA/NF-DTC and their THDs. It should be noted that the currents are less harmonious compared to the DTC, presenting with a THD value of 3.60 %; this marks improvements in the THD.

2. CONCLUSION

A neuro-fuzzy implementation on the commutation table and a genetic algorithm-based DTC PI optimization algorithm applied to DSIM were developed. This configuration was simulated in MATLAB/Simulink. This study shows that the dynamic performance of classical DTC is improved by optimizing and updating the PI coefficients KP and KI for each interval to accommodate the system's nonlinearity. The proposed GA/NF-DTC control significantly improves speed overshoot and rejection time, flux, torque ripple, and current THD.

DSIM performance brings great improvements, such as Reducing speed overshoot with and without load torque, reducing response time, and minimizing flux, ripple, and torque ripple. At the same time, there are acceptable improvements in the current THD.

Received on 10 June 2023

APPENDIX

The parameters of DSIM are given in Table 4.

Table 4
DSIM parameters

PARAMETERS	VALUES
Nominal power P_n [kW]	4.5
Stators resistance R_s [Ω]	3.72
Rotor resistance R_R [Ω]	2.12
Stators inductance L_s [mH]	22
Rotor inductance L_R [mH]	6
Mutual inductance L_m [mH]	367.2
Moment of inertia J [kg/m^2]	0.0662

REFERENCES

1. J. Henkenjohann, J. Andresen, A. Mertens, *Comparison of magnetic noise compensation techniques for dual three-phase electrically excited synchronous machines*, IEEE European Conference on Power Electronics and Applications, Germany, pp. 1–8 (2022).
2. T. Hamidatou, A. Kouzou, A. Kaddouri, A. Mida, *Fuzzy logic based speed control of indirect field oriented controlled doubly star open-end winding induction motor*, IEEE International Conference on Energy Transition and Security, Algeria, pp. 1–6 (2023).
3. R. Kianinezhad, S. Seyfossadat, V. Talaeizadeh, A. Hasani, *A new DTC of six-phase induction machines using matrix converter*, IEEE International

Conference on Advances in Computational Tools for Engineering Applications, Lebanon, pp. 127–132 (2009).
4. A. Ammar, A. Bourek, A. Benakcha, T. Ameid, *Sensorless stator field-oriented-direct torque control with SVM for induction motor based on MRAS and fuzzy logic regulation*, IEEE International Conference on Systems and Control, Algeria, pp. 156–161 (2017).
5. E. Benyoussef, S. Barkat, *Direct Torque Control based on space vector modulation with balancing strategy of dual star induction motor*, Rev. Roum. Sci. Techn.– Électrotechn. et Énerg, **67**, *1*, pp. 15–20 (2022).
6. F. Latrech, A. Ben Rhouma, A. Khedher, *Dual star induction machine driven by direct torque control using sliding mode speed controller*, IEEE International Conference on Advanced Systems and Emergent Technologies, Tunisia, pp. 1–5 (2023).
7. S. Guedida, B. Tabbache, K. Nounou, M. Benbouzid, *Direct torque control scheme for less harmonic currents and torque ripples for dual star induction motor*, Rev. Roum. Sci. Techn.– Électrotechn. et Énerg, **68**, *4*, pp. 331–338 (2023).
8. A. Gerada, N. Ekneligoda, *Direct torque control of induction motor using sliding-mode and fuzzy-logic methods*, IEEE Power& Energy Society Innovative Smart Grid Technologies Conference, USA, pp. 1–5 (2018).
9. A. Derbane, B. Tabbache, A. Ahriche, *A fuzzy logic approach based direct torque control and five-leg voltage source inverter for electric vehicle power trains*, Rev. Roum. Sci. Techn.– Électrotechn. et Énerg, **66**, *1*, pp. 15–20 (2021).
10. G. Boukhalfa, S. Belkacem, A. Chikhi, S. Benaggoune, *Direct torque control of dual star induction motor using a fuzzy-PS hybrid approach*, Applied Computing and Informatics, **18,** *1/2*, pp. 74–89 (2022).
11. A. Mansuri, R. Maurya, S. Suhel, *Reduction of common-mode voltage using zero voltage vectors in dual star asymmetrical induction motor*, IEEE Trans. on E.C., **38,** *1*, pp. 230–238 (2023).
12. K. Shah, A. Mansuri, R. Maurya, *Modified sliding mode observer-based direct torque control of six-phase asymmetric induction motor drive*, Chinese Journal of Electrical Engineering, **9**, *3*, pp. 111–123 (2023).
13. R. Bojoi, F. Farina, G. Profumo, A. Tenconi, *Direct torque control for dual three-phase induction motor drives*, IEEE Transactions on Industry Applications, **41**, *6*, pp. 433–448 (2016).
14. X. Wang, M. Elbuluk, *Neural network control of machines using genetic algorithm training*, 31st IAS Annual Meeting, IAS '96, **3**, pp. 1733–1740 (1996).
15. A. Chikhi, M. Djarallah, K. Chikhi, *A comparative study of field-oriented control and direct-torque control of induction motors using an adaptive flux observer*, SJEE, **7**, *1*, pp. 41–55 (2010).
16. K. Makhloufi, S. Zegnoun, A. Omari, I. Bousserhane, *Adaptive neuro-fuzzy-slip control of a linear synchronous machine*, Rev. Roum. Sci. Techn.–Électrotechn. et Énerg, **67**, *4*, pp. 425–431 (2022).
17. M. Zegai, M. Bendjebbar, K. Belhadri, M. Doumbia, B. Hamane, P. Koumba, *Direct torque control of induction motor based on artificial neural networks speed control using MRAS and neural PID controller*, IEEE Electrical Power and Energy Conference (EPEC), Canada, pp. 320–325 (2015).
18. I. Abdulrahman, G. Radman, *Wide-area based adaptive neuro-fuzzy SVC controller for damping interarea oscillations controller CSPR*, IEEE Transaction Canadian Journal of Electrical and Computer Engineering, **41**, *3*, pp. 133–144 (2018).
19. Y-nan. Guo, D-wei. Gong, Z. Xue, *Hybrid optimization method based on genetic algorithm and cultural algorithm*, IEEE, Proceedings of the 6th World Congress on Intelligent Control and Automation, Dalian China, pp. 3471–3475 (June 21–23, 2006).
20. A. El Idrissi, N. Zahid, M. Jedra, *Optimized DTC by genetic speed controller and inverter based neural networks SVM for PMSM*, IEEE, 2nd International Conference on Innovative Computing Technology (INTECH), pp. 392–395 (2012).
21. L. Booker, D. Goldberg, J. Holland, *Classifier systems and genetic algorithms*, Elsevier Science Publishers B.V, **40**, pp. 235–282 (1989).
22. S. Mahfud, A. Derouich, N. El Ouanjli, M. Mossa, S. Motahhir, M. El Mahfoud, S. Al-Sumaiti, *Comparative study between cost functions of genetic algorithm used in direct torque control of a doubly fed induction motor*, Applied Sciences, **12,** *17*, 8717 (2022).
23. G.H. Boukhalfa, S. Belkacem, A. Chikhi, M. Bouhentala, *Fuzzy-second order sliding mode control optimized by genetic algorithm applied in direct torque control of dual star induction motor*, Journal of Central South University, **29**, pp. 3974–3985 (2023).
24. *H. Lallouani, B. Saad, Performances of type 2 fuzzy logic control based on direct torque control for double star induction machine*, Rev. Roum. Sci. Techn. – Électrotechn. et Énerg., **65**, *1–2*, pp. 103–108 (2020).
25. A. Wang, H. Zhang, J. Jiang, D. Jin, S. Zhu, *Predictive direct torque control of permanent magnet synchronous motors using deadbeat torque and flux control*, Journal of Power Electronics, **23**, *2*, pp. 264–273 (2023).
26. R. Krohling, J. Rey, *Design of optimal disturbance rejection PID controllers using genetic algorithms.* IEEE Trans. Evol. Comput, **5**, *1*, pp. 78–82 (2001).
27. P. Maciejewski, G. Iwanski, *Study on direct torque control methods of a doubly fed induction machine working as a stand-alone dc voltage generator*, IEEE Transactions on Energy Conversion, **36**, *2*, pp. 853–862 (2021).
28. H.S. Che, E. Levi, M. Jones *et al*., *Operation of a six-phase induction machine using series-connected machine side converters*, IEEE Transactions on Industrial Electronics, **61**, *1* 164–176 (2014).